Tellus (1995), 47B, 391–413
Printed in Belgium – all rights reserved

TELLUS
ISSN 0280–6509

Long-term trend of the partial pressure of carbon dioxide (pCO_2) in surface waters of the western North Pacific, 1984–1993

By HISAYUKI YOSHIKAWA INOUE*, HIDEKAZU MATSUEDA, MASAO ISHII, KATSUHIKO FUSHIMI[1], MICHIO HIROTA[1], ICHIO ASANUMA[2] and YOSHIO TAKASUGI[3], *Geochemical Research Department, Meteorological Research Institute, Nagamine 1–1, Tsukuba, Ibaraki 305, Japan*; [1]*Marine Department, Japan Meteorological Agency, Otemachi 1–3–4, Chiyoda-ku, Tokyo 100, Japan*; [2]*Ocean Research Department, Japan Marine Science and Technology Center, Natsushima 2–15, Yokosuka, Kanagawa 237, Japan*; [3]*Research Division, Research and Investigation Bureau, Institute for Sea Training, Ministry of Transport, Kitanakadori 5–57, Naka-ku, Yokohama, Kanagawa 231, Japan*

(Manuscript received 27 December 1993; in final form 14 Feburary 1995)

ABSTRACT

The ocean is an important sink for anthropogenic CO_2 emissions, but there are only a few measurements which confirm the oceanic CO_2 uptake. Since 1981, partial pressure of CO_2 (pCO_2) in the western North Pacific (35°N–3°N, 128°E–155°E) and the overlying air have been measured periodically to clarify the seasonal and long-term trends of the oceanic carbonate system. The partial pressure of CO_2 in surface seawater (pCO_2^{sea}) observed every boreal winter during the period from 1984 to 1993 give a growth rate of 1.8 ± 0.6 μatm yr^{-1} ($n = 27$) north of 15°N and 0.5 ± 0.7 μatm yr^{-1} ($n = 23$) south of 14°N with an average of 1.2 ± 0.9 μatm yr^{-1} ($n = 50$). The rate of pCO_2^{sea} increase north of 15°N is equal to that of atmospheric CO_2 (1.8 μatm yr^{-1}) during the same period but that south of 14°N is lower. The difference in rate of pCO_2^{sea} increase is suggestive of temporal variations in ΔpCO_2 distribution. After removing the long-term trend from the pCO_2^{sea} data, the seasonal variation of pCO_2^{sea} in the western North Pacific (132°E–142°E) was evaluated with a linear regression between the pCO_2^{sea} and sea surface temperature (SST). Generally, a thermodynamic process (temperature effect) plays a predominant role in determining the seasonal variations of pCO_2^{sea}. South of 14°N, however, a clear interannual variability is significant relative to the seasonal changes if an El Niño event is accompanied by enhanced vertical mixing. The annual air-sea CO_2 flux showed a large influx of CO_2 into the ocean north of 27°N (Kuroshio Counter Current) because of a large negative ΔpCO_2 (-60 μatm) and strong wind during the winter season. Toward the south, the annual average air-sea CO_2 flux increased by 9 mmol m^{-2} day^{-1} from -8 mmol m^{-2} day^{-1} at 31°N to 1 mmol m^{-2} day^{-1} at 5°N. South of 10°N, the ocean acts as a source for atmospheric CO_2 (0.2–0.7 mmol m^{-2} day^{-1}), but this is a considerably weaker source as compared with those of the central and eastern equatorial Pacific. The observed increase of pCO_2^{sea} and the estimated air/sea CO_2 flux suggest the importance of carbon transport from the mixed layer to the intermediate/deep water in the area of Subtropical Mode Water formation, south of the Kuroshio and east of Japan.

1. Introduction

The ocean contains 50 times as much CO_2 as the atmosphere, and is an important sink for anthropogenic CO_2 emissions. However, there remain considerable uncertainties in estimates of oceanic CO_2 uptake based on global carbon cycle models (IPCC 1990). At locations remote from fossil fuel combustion and local vegetation, measurements of atmospheric CO_2 show evidence

* Corresponding author.

of a persistent increase in concentration. The record maintained by the Scripps Institution of Oceanography at Mauna Loa Observatory shows a 12% increase during the period from 1958 to 1989 (Keeling et al., 1989). Because the increase of carbon in the ocean is relatively small compared with that in the air, there are only a few measurements which confirm the accumulation of CO_2 in the ocean. In sea water, most dissolved inorganic carbon is in the forms of bicarbonate and carbonate ions and less than 1% is aqueous CO_2, expressed as $H\mathrm{pCO}_2^{\mathrm{sea}}$, where H is the Henry's law constant and $\mathrm{pCO}_2^{\mathrm{sea}}$ is the partial pressure of CO_2. If there is a net addition of CO_2 to the ocean, the mole fraction of each of the dissolved inorganic carbon species varies from its original value because CO_2 acts as a weak acid in water. The relationship between $\mathrm{pCO}_2^{\mathrm{sea}}$ and dissolved inorganic carbon concentration (TCO_2) is conventionally expressed by the homogeneous buffer factor (Revelle and Suess, 1957):

$$\beta = [(\delta \mathrm{pCO}_2^{\mathrm{sea}}/\mathrm{pCO}_2^{\mathrm{sea}})/(\delta \mathrm{TCO}_2/\mathrm{TCO}_2)], \quad (1)$$

where $\delta\mathrm{pCO}_2^{\mathrm{sea}}$ and $\delta\mathrm{TCO}_2$ are small changes in $\mathrm{pCO}_2^{\mathrm{sea}}$ and TCO_2, respectively. This equation gives the CO_2 uptake capacity of ocean water and reported values (Sundquist, 1979; Wagner, 1979) indicate that the relative change in $\mathrm{pCO}_2^{\mathrm{sea}}$ is about order of magnitude larger than that of TCO_2.

The net flux of CO_2 between the sea and the air (Fx) is given by the product of the difference in pCO_2 between the sea and the air ($\Delta\mathrm{pCO}_2 = \mathrm{pCO}_2^{\mathrm{sea}} - \mathrm{pCO}_2^{\mathrm{air}}$) and the gas transfer coefficient (E). Changes in $\Delta\mathrm{pCO}_2$ stem mainly from the $\mathrm{pCO}_2^{\mathrm{sea}}$ being controlled by mixing dynamics of the upper ocean, thermodynamic processes, CO_2 exchange between the sea and the air, and biological processes. To quantify the air-sea CO_2 flux at a global scale, world maps have been drawn by compiling existing $\mathrm{pCO}_2^{\mathrm{sea}}$ data (Keeling, 1968; Broecker et al., 1986; Tans et al., 1990). The $\mathrm{pCO}_2^{\mathrm{sea}}$ data, however, are not sufficient to depict the temporal and spatial variations; more $\mathrm{pCO}_2^{\mathrm{sea}}$ data and analyses of the factors controlling $\mathrm{pCO}_2^{\mathrm{sea}}$ change are essential for better understanding of air-sea CO_2 flux.

Since 1981 simultaneous measurements of atmospheric and oceanic pCO_2 have been made periodically along the same transects (34°N to 0° along 137°E and back to Naha; 25°N, 128°E) aboard the Japan Meteorological Agency (JMA) ship R/V Ryofu-maru. The cruise tracks where repeated pCO_2 measurements were made are drawn in Fig. 1, and arrival dates for selected geographical positions for repeated transects are listed in Table 1. Prior to 1989, the Meteorological Research Institute (MRI) made these observation and in 1990 the JMA took over following the start of operational pCO_2 observations aboard the R/V Ryofu-maru which uses basically the same analytical system as that of MRI (Hirota, 1989). Besides repeated measurements along the same cruise tracks, measurements at different geographical positions and times have been made to elucidate temporal and spatial variations in atmospheric and oceanic pCO_2.

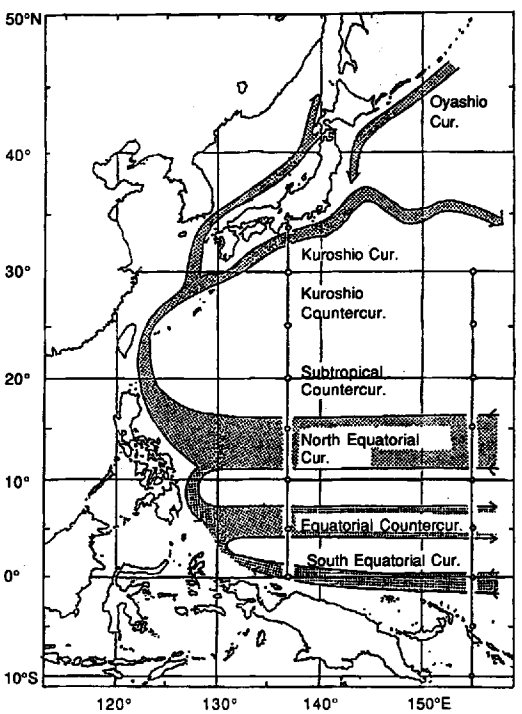

Fig. 1. Repeated transects where $\mathrm{pCO}_2^{\mathrm{sea}}$ measurements were made since 1981. Open circles indicate the major oceanographic stations, where seawater samples from surface to the bottom were taken by CTD casts for measurement of oxygen, TCO_2, nutrients, salinity and so on. South of 32°N along 137°E the oceanographic stations were located at every 1° intervals, and CTD casts to 1000 (or 2000) dbar were obtained. The typical pattern of the major currents in the western North Pacific are indicated.

Table 1. *Date of arrival at the indicated geographical position by the R/V Ryofu-maru*

Winter cruises

Year	34°N, 137°E	3°N, 137°E	25°N, 128°E	7°N, 135°E	25°N, 130°N
1984	20 Jan.	31 Jan.	8 Feb.		
1985	18 Jan.	29 Jan.	6 Feb.		
1986	19 Jan.	30 Jan.	7 Feb.		
1987	15 Jan.	25 Jan.	2 Feb.		
1988	16 Jan.	29 Jan.	4 Feb.		
1989	20 Jan.	29 Jan.	6 Feb.		
1990	20 Jan.	1 Feb.	7 Feb.		
1991	19 Jan.	30 Jan.	4 Feb.		
1992*	19 Jan.	1 Feb.		3 Feb.	16 Feb.
1993*	20 Jan.	2 Feb.		4 Feb.	14 Feb.

Summer cruises

Year	30°N, 155°E	0°, 155°E		
1987	14 June	22 June		
1990	19 June	28 June		
1991	10 June	19 June		
1992	14 June	23 June		
Year	3°N, 137°E	11°N, 137°E	11°N, 137°E	34°N, 137°E
1987	2 July	4 July	17 July	25 July
Year	3°N, 137°E	13°N, 137°E	13°N, 137°E	34°N, 137°E
1990	7 July	11 July	24 July	30 July
1991	29 June	2 July	16 July	23 July
1992	2 July	5 July	20 July	26 July

* Oceanographic observation along 130°E north of 8°N began in 1992.
For 1981–1983, see Inoue et al. (1987).

Some results have been reported earlier: in the area of the Kuroshio Current and the Kuroshio Counter Current (north of 27°N), the pCO_2^{sea} is low in comparison with that in the air (-60 μatm) in winter and increases to a level somewhat higher (10–20 μatm) than that of atmospheric CO_2 in summer (Inoue and Sugimura, 1992). In the western equatorial Pacific the pCO_2^{sea} is slightly supersaturated with respect to atmospheric CO_2 (0–20 μatm), and was perturbed considerably by the 1982/83 El Niño event (Fushimi, 1987; Inoue et al., 1987). Long-term increases of pCO_2^{sea} in the western North Pacific and in the Southern Ocean south of Australia nearly equal to the increase in the atmosphere were detected based on the data collected during boreal winter in 1969 and 1984 (Inoue and Sugimura, 1988a). This increase is, however, calculated from the two sets of pCO_2^{sea} measurements collected over a decade apart. In order to clarify the changing carbon cycle in surface seawater, systematic and repeated measurements are required because the long-term variation of the carbonate system is small compared with its short-term variations.

Here, we report the pCO_2 in the western North Pacific (35°N–0°, 125°E–155°E) and overlying air along with other oceanographic data and discuss the temporal variation in pCO_2^{sea} (TCO_2) and CO_2 flux between the sea and the air. The pCO_2 data which were reported in Inoue and Sugimura (1992) are available from the present authors or from the WMO World Data Center for Greenhouse Gases (JMA), and those presented in this paper will be available on a floppy disk in the near future.

2. Sampling and analytical methods

2.1. Measurements of oceanic and atmospheric CO_2, 1981–1986

The CO_2 concentrations in dry air (xCO_2^{air}) and in dry air equilibrated with seawater (xCO_2^{sea}) were measured using the same basic analytical

system described by Miyake et al. (1974). The system consists primarily of a non-dispersive infra-red gas analyzer (NDIR analyzer, Beckman model 315A), a showerhead-type equilibrator, diaphragm pumps, a series of valves, an electro-mechanical timing device, an electric dehumidifier, a chemical desiccant column ($Mg(ClO_4)_2$), and associated instrumentation. Air was pumped at 10 l/min from an inlet installed at jackstaff on the bow of the ship. Aliquots of sample air (0.5 l/min) were introduced into the sample cell of the NDIR analyzer. Seawater was pumped at 10 l/min up from the bottom of the ship, 4 m below the surface. Half of this water flow rained through the equilibrator.

The effect of the seawater temperature rise between the equilibrator and surface seawater was corrected using the equation given by Gordon and Jones (1973).

$$\frac{\delta pCO_2}{\delta t} = 4.4 \times 10^{-2}(pCO_2) - 4.6 \times 10^{-6}(pCO_2)^2. \quad (2)$$

Prior to entering the sample cell of the NDIR analyzer all gases were dried by passing them through the electric dehumidifier and the $Mg(ClO_4)_2$ column. At 1-h intervals, 2 calibrated working standard gases (250 ppm and 450 ppm CO_2 in N_2) were passed in succession through the sample cell of the NDIR analyzer at 0.5 l/min for 5 min each. The other working standard gas (350 ppm) was usually used once a day to estimate the curvature between concentration and output voltage of NDIR analyzer. To measure xCO_2^{air} and xCO_2^{sea} precisely, the gas pressure and temperature in the sample cell of NDIR analyzer should be the same as those for the standards.

When oceanic CO_2 was measured, air circulated in a closed loop (ca. 2 l), consisting of the NDIR analyzer, the equilibrator, the diaphragm pump, and the desiccant unit. Gas circulation by the diaphragm pump led to pressure changes in the various parts of the closed loop. Changes in pressure in the sample cell are dependent on the flow rate and the order of connections among the respective parts. For example, when the diaphragm pump is placed between the electric dehumidifier and the equilibrator, the pressure in the sample cell increased, but when between the equilibrator and the NDIR analyzer, the pressure decreased.

For the shipboard measurements made in 1981 and 1982, there is evidence suggesting that pressure affected the observed xCO_2^{sea}. Unfortunately, this technical problem was overlooked. Because the gas flow rate (0.55 l/min) was almost equal to that of the working standard gases, the pressure in the sample cell during oceanic CO_2 measurement was assumed to be equal to that during working standard gas measurements. There are only a few data which are necessary to correct pressure effect during oceanic CO_2 measurements. We estimated the pressure effect by comparing the output voltage of NDIR analyzer during the gas flow with that of stoppage of gas flow. The effect of pressure is estimated to have been 3.1, 4.8 and 1.7 ppm in 1981, and 7.7 ppm in 1982. The data points are too few to estimate the pressure effect quantitatively. Therefore, the data obtained in 1981 and 1982 are not used to estimate the temporal variations in pCO_2^{sea} but rather to depict the pCO_2^{sea} spatial variation and to indicate that pCO_2^{sea} is explicitly controlled by large scale and permanent processes (Poisson et al., 1994).

During the cruise of November 1982, seawater flowed over the air sample outlet in the equilibrator and the sample cell of the NDIR analyzer was flooded. This flooding was caused by air leaking into the electric dehumidifier and the resulting pressure decrease in the equilibrator. Because of this serious malfunction of the system, we replaced the electric dehumidifier, the solenoid valves, the diaphragm pump, connections, etc. During the cruise in January and February 1983, we adjusted the pressure in the equilibrator by changing the gas flow rate, the length of pipe, and the order of connections for the respective parts to keep the water level constant in the equilibrator. For this reason the oceanic and atmospheric CO_2 data for January 1983 between 35°N and 34°N, and 32°N and 29°N are missing (Inoue et al., 1987). After the correction of the pressure effect problem, 33°N data were obtained. This adjustment resulted in a decrease of the pressure effect on xCO_2^{sea}. In January and February 1983, a decrease of output voltage due to the stoppage of air flow in the closed loop (1.2 ± 0.3 ppm, $n = 8$) is considered to be the same as that for atmospheric CO_2 (1.0 ± 0.2 ppm, $n = 18$). For the period from 1984 to 1986, there is no indication that the pressure effect on xCO_2^{sea} has changed. Therefore, we will use the pCO_2^{sea} data reported earlier (Fushimi, 1987; Inoue et al., 1987).

At the end of February 1985, we started to improve our analytical system. We decided to use four different CO_2 standard gases to measure xCO_2^{air} and xCO_2^{sea} instead of three (Inoue et al., 1987). The 4 standard gases were introduced into the NDIR analyzer's cell successively every hour. This decreased the available time for measuring xCO_2^{air} and xCO_2^{sea}. The equilibrator was improved by decreasing the pore size of the shower and increasing the number of pores. The time until equilibrium is established depends on the difference in pCO_2 between the air and the seawater in the equilibrator. Because the air in the equilibrator (1.9 l) exchanges CO_2 with seawater during the measurements of CO_2 standard gases and atmospheric CO_2, most of the air in the closed loop (2 l) attains equilibrium prior to the oceanic CO_2 measurements. The difference in pCO_2 between the air in the closed circuit and the seawater is usually less than 20 μatm. It needs less than 10 min to re-eqilibrate. 20 min was allocated for each measurement of the standard gases, xCO_2^{air} or xCO_2^{sea}. We used this system for the period from May 1985 to July 1986 (Fig. 3 in Inoue et al., 1987).

2.2. *Measurements of oceanic and atmospheric CO_2, 1987-1993*

In January 1987, we introduced a new system to measure xCO_2^{air} and xCO_2^{sea} (Inoue and Sugimura, 1988a; Inoue and Sugimura, 1992). As this system was reported earlier, only a short description of the technique is given here.

Changes in both pressure and temperature in the NDIR analyzer's cell (Beckman model 864, model 865, and model 880) and water vapor of sample air are factors which affect the determination of xCO_2^{air} and xCO_2^{sea}. To avoid the effects of room temperature change, the NDIR analyzer was installed in a box placed in an air conditioned room. During a step change in room temperature, for example from 25°C to 22°C, the temperature in the box varies by less than 0.1°C, which maintains the temperature in the NDIR analyzer constant. 20 s before signal integration (A/D conversion), the flow of the respective gases was stopped and the outlet valve opened (open-end configuration) to equilibrate the temperature and pressure in the NDIR analyzer's cell. A perma-pure dryer tube (Perma Pure Ltd.) between the electric dehumidifier and the chemical desiccant column ($Mg(ClO_4)_2$) to remove the water vapor from sample gas was introduced. Dry air was supplied to the perma-pure dryer via the diaphragm pump, the heatless-dryer (CKD) in which zeolite is used to remove water vapor, and the mass flow controller. The water vapor of sample gas is removed by molecular diffusion through a film made of ion exchange resin. The dew point of sample air flowing at 0.6 l/min is lower than 2°C at the outlet of the electric dehumidifier and lower than −40°C at the outlet of the perma-pure dryer.

Fluctuations of electric power frequency and voltage on the ship also affect the xCO_2^{air} and xCO_2^{sea} determination. We have divided the electric lines in the NDIR analyzer into two parts, one for the unit requiring constant voltage and frequency and the other for the insensitive units such as those for heating, the electric fan etc. A voltage and frequency stabilizer was used for the former unit (Takasago AF330).

The precision of replicate analyses with this system in our laboratory on land is better than 0.05 ppm for Beckman models 865 and 880, and better than 0.2 ppm for Beckman model 864 (Inoue and Sugimura, 1992).

In January 1990, the TCO_2 measured by gas chromatography at every 5° of latitude along 137°E was within the range from 1914 μmol kg^{-1} to 1998 μmol kg^{-1} (The Results of Oceanographic Observations, 1990). The precision of TCO_2 determinations on board is estimated to be 5–6 μmol kg^{-1}.

2.3. *CO_2 standard gas*

Our standard gases are classified into three categories; primary, secondary and working. During the period from January 1981 to April 1986, CO_2 in N_2 mixtures were used as working reference gases, for calibrations before and after the cruise relative to secondary standards. These CO_2 in N_2 gas mixtures were used because their CO_2 concentrations remain highly stable with time. The secondary standard gases were calibrated at least twice annually against primary standard gases, prepared gravimetrically by Takachiho Co. Ltd. Both primary and secondary standard gases are composed of CO_2 in synthetic air with no argon. The NDIR analyzer used for shipboard measurements (Beckman 315A) was employed to calibrate the working reference gases.

Therefore, the observed value is based on CO_2 mole fraction in synthetic air.

Since April 1987, CO_2 standard gases (CO_2 in natural air) made by Nippon Sanso have been used as primary, secondary, and working standard gases. The primary standard gases, which were made gravimetrically following the same procedures reported by Tanaka et al. (1987), provide a scale (MRI87) developed independently of the mole fraction scale of Takachiho and that of WMO (Nakazawa et al., 1992). The relationship between the MRI87 scale and the Takachiho scale is given by:

$$xCO_2^{NS} = 0.247 + 1.028(xCO_2^{TK}) - 7.650 \times 10^{-5}(xCO_2^{TK})^2 \quad (3)$$

where xCO_2^{NS} is the mole fraction in dry air based on the MRI87 scale and xCO_2^{TK} is that based on the Takachiho scale (Inoue and Sugimura, 1992).

We participated in the CO_2 round robin intercomparison conducted in 1991 and 1992. The results of our analysis system show good agreement with the 1985 WMO mole fraction scale within the range from 330 ppm to 370 ppm. Reports of this intercomparison will be published in the near future (Peterson, private communication).

The JMA has been using four CO_2 working reference gases ranging from 290 to 400 ppm to conduct operational observations from the R/V Ryofu-maru. These working standard gases were calibrated before and after each cruise against the secondary standard gases, which are calibrated twice annually against the 1985 WMO standard gases. We have sent our cylinders to the JMA once annually to compare our MRI87 scale with the 1985 WMO scale. The relationship between the MRI87 scale and the 1985 WMO scale is given by:

$$xCO_2^{WMO} = 5.410 + 0.975(xCO_2^{NS}) + 2.530 \times 10^{-5}(xCO_2^{NS})^2, \quad (4)$$

where xCO_2^{WMO} is the mole fraction based on the 1985 WMO scale. However, this relationship is only tentative and may change considerably in the future. The concentration used in this intercomparison ranged from 290 ppm to 400 ppm. In this paper we report CO_2 concentrations based on the 1985 WMO scale as calculated by eq. (4).

2.4. *Selection of atmospheric and oceanic CO_2 concentration data*

The objective of selecting data is to identify xCO_2^{air} and xCO_2^{sea} values which are not affected by local sources and sinks. Since air CO_2 variations with a frequency from a few minutes to a few tens of minutes are clearly due to local contamination, we first rejected data showing instability of CO_2 concentrations within a few tens of minutes, readily seen in an analog recording of the NDIR analyzer strip chart recorder output. If changes in the CO_2 concentration between 1-hour intervals or a few tens of kilometers were large, we rejected those CO_2 values based on the assumption that CO_2 concentrations in representative air should change by only small amounts over such short distances and times. The amount of CO_2 change is, however, dependent on both time and position. For example, a prevailing northwest wind off the coast of Japan during the winter, which sweeps over the Asian continent and Japan, leads not only to high concentrations but also to high variability as compared with concentrations at remote stations (Inoue et al., 1987; Inoue and Sugimura, 1992). Here, we simply rejected xCO_2^{air} data which varied by more than ± 1 (or 2) standard deviations (σ) for each degree of latitude or longitude. Visual inspection of the remaining data sometimes reveals that temporal variations over hours at an oceanographic station are large in comparison with those measured under steam, probably due to local contamination. These values have been rejected unless the standard deviation of the CO_2 concentration became equal to or less than the standard deviation when the ship was underway. After examination of the data with respect to oceanographic parameters, some of the xCO_2^{sea} measurement data, those exceeding 3σ from the latitudinal or longitudinal average, were excluded as unrepresentative.

Our selection scheme removed 20% of the atmospheric CO_2 values and 6% of the oceanic CO_2 values out of the total data ($n = 18853$ for each) gleaned by the MRI cruises during the period from January 1981 to March 1993. The standard deviation of average xCO_2^{air} at each latitude is typically within the range from 0.1 ppm to 0.8 ppm for the period from 1981 to 1986, and from 0.1 ppm to 0.4 ppm for the period from 1987 to 1993. The dispersion in the data is dependent on natural variability, the NDIR analyzer, weather

conditions, the power supply, etc. On the basis of our data it is difficult to extract the natural variability. As reported earlier (Inoue and Sugimura, 1992), measurements of atmospheric CO_2 show good agreement with those of baseline stations as far as conditions on board permit.

2.5. CO_2 flux between the sea and the air in 1990

CO_2 flux (Fx) can be computed as;

$$Fx = kS_1 \Delta pCO_2 = E \Delta pCO_2, \quad (5)$$

where k is the air-sea gas transfer piston velocity for CO_2, and S_1 is the solubility of CO_2 in seawater (Weiss, 1974). Liss and Merlivat (1986) and Etcheto and Merlivat (1988) suggested that k (cm h^{-1}) for CO_2 depends on the wind speed and the Schmidt number (Sc):

$$k = 0.17 U_{10} (Sc_{20}/Sc)^{2/3}, \quad 0 < U_{10} \leqslant 3.6 \text{ m s}^{-1}, \quad (6a)$$

$$k = [2.85 U_{10} - 9.65](Sc_{20}/Sc)^{1/2}, \quad 3.6 < U_{10} \leqslant 13 \text{ m s}^{-1}, \quad (6b)$$

$$k = [5.9 U_{10} - 49.3](Sc_{20}/Sc)^{1/2}, \quad U_{10} > 13 \text{ m s}^{-1}, \quad (6c)$$

where U_{10} is the wind speed 10 m above the sea surface and Sc_{20} is the Schmidt number of seawater at 20°C (Wanninkhof, 1992).

Tans et al. (1989) have reported that:

$$E = 0.016(U - 3), \quad (7)$$

where U is the wind speed and E (moles of CO_2 m^{-2} yr^{-1} μatm^{-1}) is taken to be zero for $U \leqslant 3$ m s^{-1}. Taking into account the characteristics of the wind data set and chemical enhancement, Wanninkhof (1992) has suggested some formulas. Since we use monthly mean wind speed data provided by JMA (1990), we adopted a formulation for k corresponding to the long-term wind speed (U_{av}) data:

$$k = 0.39 U_{av}^2 (Sc_{20}/Sc)^{1/2}. \quad (8)$$

The monthly mean wind speed was compiled for every 2° by 2° pixel on the basis of observations gathered on board during the period from 1971 to 1980 (JMA, 1989). In this paper we will use eqs. (5)–(8) for the air-sea CO_2 flux calculations.

3. Results and discussion

3.1. Long-term trend of pCO_2 along 137°E during boreal winter

The distribution of pCO_2^{sea} during January and February 1990 shows a pattern (Fig. 2) similar to that reported earlier (Inoue et al., 1987; Fushimi, 1987). The pCO_2^{sea} off the coast of central Japan was low in comparison with the pCO_2^{air}, and tends to increase towards the south. South of 5°N, ΔpCO_2 in surface seawater became positive. The pCO_2^{air} was slightly higher near the coast of Japan, and nearly constant south of 15°N (Inoue and Sugimura, 1992). The pCO_2^{sea} data from the periodically repeated observations were digitized at 0.1-year intervals and 0.3°-latitude intervals by the cubic spline function to observe the patterns of latitudinal and temporal variation. The highly smoothed surfaces obtained (Figs. 3, 4) show that the distribution of pCO_2^{sea} maintains characteristic features over a decade which are controlled by large-scale and permanent processes (Poisson et al., 1993).

El Niño events alter the distribution of pCO_2^{sea} in the equatorial Pacific (Feely et al., 1987; Inoue and Sugimura, 1988b, 1992; Wong et al., 1993). The pCO_2^{sea} in the western equatorial Pacific increased considerably due to the enhancement of vertical mixing during 1982/83 El Niño events (Fushimi, 1987; Inoue et al., 1987), although during the 1986/87 El Niño event pCO_2^{sea} was almost the same as that typical of non-El Niño periods (Inoue and Sugimura, 1988b; Inoue and Sugimura, 1992). In January 1987 the SST anomalies are close to zero in the western equatorial Pacific (Fig. 5), which suggests that changes in vertical mixing at that time were less than those of the 1982/83 El Niño event. Since 1991, the SST anomalies in the western equatorial Pacific have changed periodically, becoming negative in winter and almost zero in summer (Fig. 5). After 1991 the pCO_2^{sea} in the western equatorial Pacific observed during winter increased by 20–30 μatm in comparison with that of non-El Niño periods due to the effect of vertical mixing (Figs. 3, 4).

North of 30°N, the pCO_2^{sea} and other oceanographic parameters changed considerably from year to year. For example, the concentrations of nutrients ($NO_2^- + NO_3^-$) in January 1990 decreased monotonously from 33°20'N to 30°N (Fig. 2), while in January 1989 they decreased

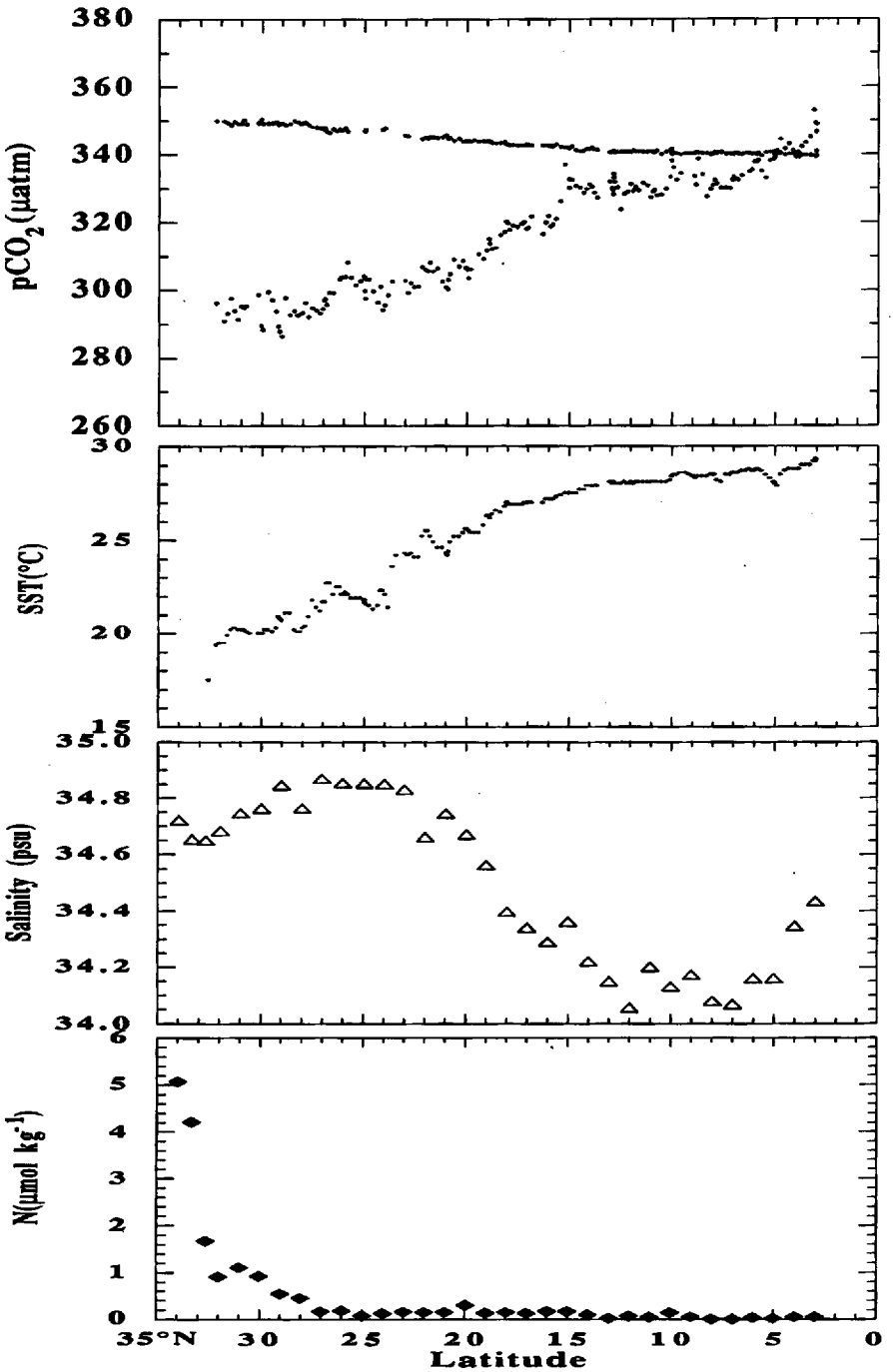

Fig. 2. Latitudinal distribution of pCO_2^{sea}, pCO_2^{air}, SST, salinity and the concentration of $NO_2^- + NO_3^-$ along 137°E in January 1990.

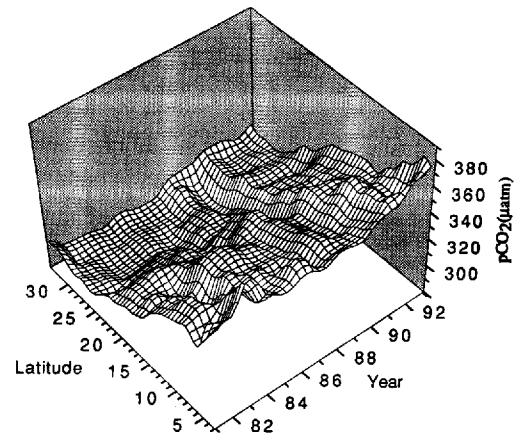

Fig. 3. Variations in pCO_2^{sea} along 137°E during the period from 1981 to 1993. Measurements of pCO_2^{sea} were made at the same time (late January) each year. The pressure effect on the CO_2 concentration in the air equilibrated with seawater were corrected for the 1981 and 1982 data (-1.2 μatm in 1981 and -6.7 μatm in 1982).

steeply by 6.3 μmol/kg between 33°20'N and 32°40'N (data not shown). These changes were presumably caused by effects of the Kuroshio meander, mixing with coastal water, the vertical mixing, and changes in biological activities. The Kuroshio, the western boundary current of North Pacific, takes one of two different courses as it flows along the south coast of the Japanese islands: one of these is straight, parallel to the south coast of Japan (Fig. 1), and the other, the large meander course, is accompanied by the cold water mass off the coast of central Japan (Ishii et al., 1983). The Kuroshio meander occurred for the periods between November 1981 and August 1984, December 1986 and September 1988, and December 1989 and June 1991 (Monthly Ocean Report, 1993). When the Kuroshio meanders, the axis of the Kuroshio often reaches around 30°N south of central Japan (Kawabe, 1990). A full discussion of the temporal and spatial changes in pCO_2^{sea} due to the Kuroshio meander is beyond the scope of the present paper. In order to focus on the long-term trends of the oceanic carbonate system caused by CO_2 exchange between the sea and the air, we will omit the data for pCO_2^{sea} observed in the western equatorial Pacific from January 1991 to January 1993 and north of 30°N.

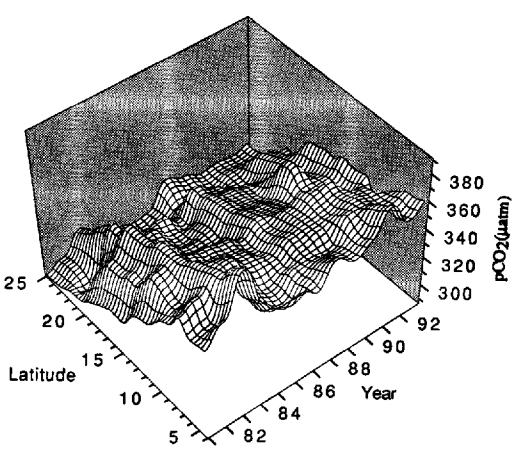

Fig. 4. Variations in pCO_2^{sea} in surface seawater from 3°N, 137°E to Naha (25°N, 128°E). Measurements of pCO_2^{sea} were made at the same time (late January) each year. Because the JMA started measurements of pCO_2^{sea} along 130°E (north of 7°N) since 1992, the longitude and time of year for these data are slightly different from those of others. In 1989 we could not measure pCO_2^{sea} north of 7°N because of a malfunction of our system.

As seen in Fig. 2, the pCO_2^{sea} scattered relatively less and the concentrations of $NO_2^- + NO_3^-$ were close to zero in the area between the Subtropical Counter Current and the South Equatorial Current (27°N–3°N). Every year the standard deviation for the mean pCO_2^{sea} value (1σ) at each latitude is usually in the range from 1 μatm to 5 μatm. Murphy et al. (1993) have reported that the interannual variability of ΔpCO_2 measured at the same time (within a 30-day period) over 4 years along 50°N in the North Pacific can be significant relative to seasonal variability. Wong et al. (1991) have reported that the interannual variation in pCO_2^{sea} at Ocean Station P(50°N, 145°W) were caused by effects other than CO_2 exchange between the sea and the air. In the area between 30°N and 3°N, however, seasonal variations in pCO_2^{sea} can be well approximated by SST (see section 3.4) and no clear difference in the pattern of pCO_2^{sea} distribution was found for the period from 1981 to 1993 except during El Niño events (Figs. 3, 4). Therefore, the air-sea CO_2 exchange in the area between 30°N and 3°N is expected to play a relatively important role in determining the interannual variability of pCO_2^{sea}.

Assuming a linear long-term trend, the pCO_2^{sea} data for each latitude were fitted to a linear function by the least squares method. The pCO_2^{sea} data in 1983 were not included in the calculations of the long-term trend because pCO_2^{sea} south of 17°N

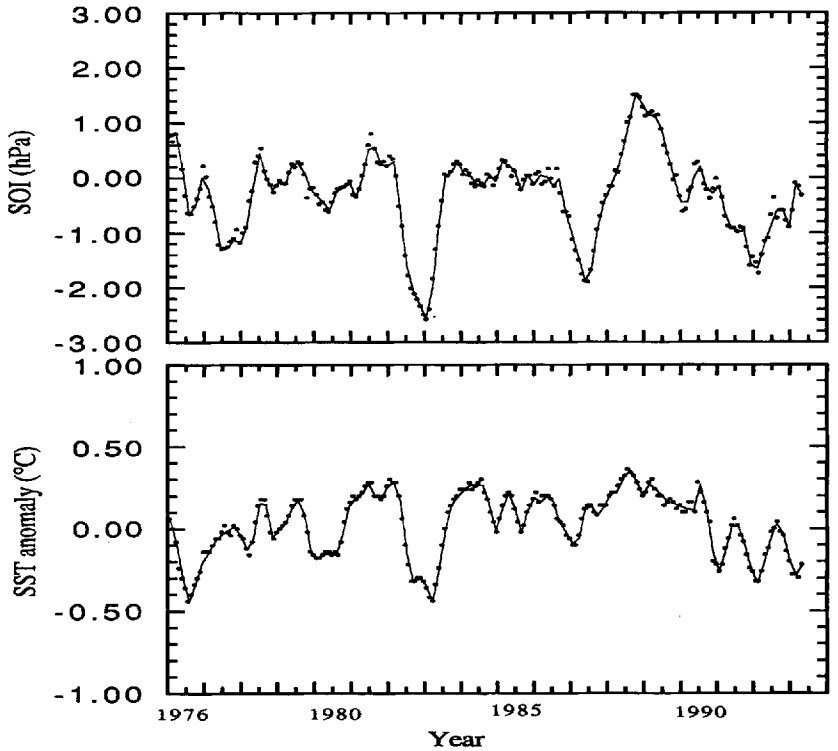

Fig. 5. SOI and SST anomalies in the area 14°N–0° and 130°E–137°E (region of the north equatorial current, the equatorial counter current, and the south equatorial current: Monthly Ocean Report 1993).

was perturbed by the 1982/83 El Niño event. If we include the pCO_2^{sea} data north of 18°N in 1983, no substantial change in the increase rate occurred. The calculated increase rate is 1.4 ± 0.9 μatm yr^{-1} ($n = 28$) along 137°E and 1.0 ± 0.9 μatm yr^{-1} ($n = 22$) for northbound cruises (Table 2), implying a clear increase in pCO_2^{sea} during this period. Only a few studies report the long-term trend of pCO_2^{sea} or ΔpCO_2 on the basis of on board measurements (Inoue and Sugimura, 1988; Goyet and Peltzer, 1994). The present study shows a discontinuity in this pCO_2^{sea} growth rate: north of 15°N the pCO_2^{sea} growth rate is 1.8 ± 0.6 μatm yr^{-1} ($n = 26$), while it is 0.5 ± 0.7 μatm yr^{-1} ($n = 22$) south of 14°N. The correlation coefficient between observed pCO_2^{sea} and year (time) varied considerably from place to place, which ranged from -0.03 to 0.83 along 137°E and from -0.69 to 0.70 for the northbound cruise track (data not shown), indicating the existence of processes producing short-term and/or interannual variations other than CO_2 exchange between the sea and the air. During the same period, the pCO_2^{air} south of 15°N along 137°E has increased from 331 μatm to 346 μatm with an average increase rate of 1.8 μatm yr^{-1}. While, the apparent growth rate of pCO_2^{sea} north of 15°N is equal to that of the atmospheric CO_2, that south of 14°N has been slower (Table 2). The spatial difference in growth rate of pCO_2^{sea} is suggestive of long-term variations in ΔpCO_2 as reported based on a carbon cycle model (Volk and Bacastow, 1989). To confirm that the long-term variations in ΔpCO_2 are caused by air-sea CO_2 exchange, however, more pCO_2^{sea} data should be collected because of the large short-term and interannual variabilities of pCO_2^{sea}.

3.1.1. Normalization of pCO_2 to account for thermodynamic and biological effects. As described above, the mixing dynamics of the upper ocean, thermodynamic processes, air-sea CO_2 fluxes and biological activities are factors affecting pCO_2^{sea}. In order to evaluate whether the long-term trend of

Table 2. *Growth rate of observed pCO_2^{sea} (Gr^{obs}) and that of normalized pCO_2^{sea} (Gr^{nor}) in the western North Pacific, 1984–1993; numbers of observation (No.) and correlation coefficients (r) are given for normalized pCO_2^{sea}*

	Along 137°E and northbound cruise to Naha Boreal winter					Along 137°E Boreal summer			Along 155°E Boreal summer		
Latitude N	*Gr^{obs} μatm/yr	+Gr^{obs} μatm/yr	Gr^{nor} μatm/yr	No.	r	Gr^{nor} μatm/yr	No.	r	Gr^{nor} μatm/yr	No.	r
30	1.9		1.9	10	0.80						
29	1.5		0.6	10	0.30						
28	2.0		1.7	10	0.51						
27	2.0		1.9	10	0.77						
26	2.9		0.0	10	0.01						
25	2.5	1.4	3.2	10	0.68						
24	2.3	1.4	−0.0	10	−0.01						
23	2.5	1.0	−1.1	10	−0.34						
22	2.5	0.9	0.4	10	0.12						
21	2.1	0.5	1.1	10	0.38						
20	2.0	1.0	1.9	10	0.73						
19	2.7	1.0	2.4	10	0.69	2.6	4	0.66			
18	2.4	1.2	2.3	10	0.65	2.4	4	0.91			
17	2.1	1.6	2.1	10	0.70	3.3	4	0.77			
16	1.6	2.5	2.2	10	0.65	3.6	4	0.85			
15	1.2	2.6	2.6	10	0.76	2.6	4	0.88	2.8	4	0.65
14	−0.1	−0.6	1.0	7	0.41	3.5	4	0.82	2.4	4	0.87
13	0.0	−1.5	1.1	7	0.39	1.3	4	0.56	2.5	4	0.85
12	0.1	0.9	1.4	7	0.54	1.5	4	0.49	1.1	4	0.54
11	0.2	0.6	0.5	7	0.22	1.5	4	0.63	1.6	4	0.83
10	0.4	0.5	0.1	7	0.07	0.8	4	0.38	2.5	4	0.69
9	0.4	0.2	−0.0	7	−0.03	−0.1	4	−0.04	2.3	4	0.93
8	0.3	1.5	0.9	7	0.33	1.4	4	0.37	2.9	4	0.83
7	0.3	2.0	1.1	7	0.50	0.6	4	0.38	2.0	4	0.88
6	1.3	1.8	1.2	7	0.44	−0.4	4	−0.11	2.5	4	0.71
5	0.7	1.0	0.7	7	0.28	2.0	4	0.61	3.5	4	0.93
4	0.6	0.2	−0.4	7	−0.18	−1.5	4	−0.78	1.1	4	0.54
3	0.7		−1.1	7	−0.29	0.4	4	0.08	1.3	4	0.61
2									0.0	4	0.02
1									1.2	4	0.60
0									2.0	4	0.79
average	1.4 ± 1.0	1.0 ± 0.9	1.0 ± 1.1			1.5 ± 1.4			2.0 ± 0.9		

* Along 137°E.
\+ From 4°N, 136°E to Naha (25°N, 128°E).

pCO_2^{sea} has been caused by oceanic CO_2 uptake, the pCO_2^{sea} changes due to the thermodynamic and biological effects have been removed from the observed pCO_2^{sea} data. To estimate the changes due to temperature, salinity and biological processes, we first calculated the mean values of SST, salinity, and concentration of $NO_2^- + NO_3^-$ at the oceanographic stations at 1°-latitude intervals south of 32°N along 137°E, for the period from 1984 to 1993. The pCO_2^{sea} at each latitude was normalized to the average SST and salinity using equations for the temperature (eq. (2)) and salinity dependence of pCO_2^{sea} (Weiss et al., 1982):

$$\frac{\delta(\ln pCO_2^{sea})}{\delta S} = 0.08620 - 1.2726 \times 10^{-3} S, \qquad (9)$$

where S is salinity.

Assuming the Redfield ratio (C:N:P = 106:16:1)

to scale changes in $NO_2^- + NO_3^-$ to the uptake of TCO_2 and temperature dependence of the buffer factor (Sundquist, 1979), changes in pCO_2^{sea} due to the biological activity were estimated by eq. (1). TCO_2 at each latitude was obtained by linear interpolation of data measured at 5-latitude intervals. The TCO_2 in surface seawater along 137°E ranged from 1914 μmol kg^{-1} to 1998 μmol kg^{-1}. Other values of TCO_2 in the realistic range from 1900 μmol kg^{-1} to 2000 μmol kg^{-1} (Takahashi et al., 1993) result in variations in pCO_2^{sea} change of less than 0.5 μatm due to biological activity.

The normalized pCO_2^{sea} (Fig. 6) shows a pattern similar to that seen in Fig. 3. The increase of pCO_2^{sea} tends to be large north of the Subtropical Counter Current (15°N), and small in the North Equatorial Current, the Equatorial Counter Current and the South Equatorial Current (Table 2). As discussed in Subsection 3.3, the region north of the Subtropical Counter Current acts as a sink for atmospheric CO_2, while the North Equatorial Current and the Equatorial Counter Current act as either weak sinks or sources. The average oceanic CO_2 increase rate along 137°E is 1.0 ± 1.1 μatm yr^{-1} ($n = 28$). However, the correlation coefficient in Table 2 is no higher than that of the relationship between observed pCO_2^{sea} and time (year), suggesting that there remain other processes affecting the inter-

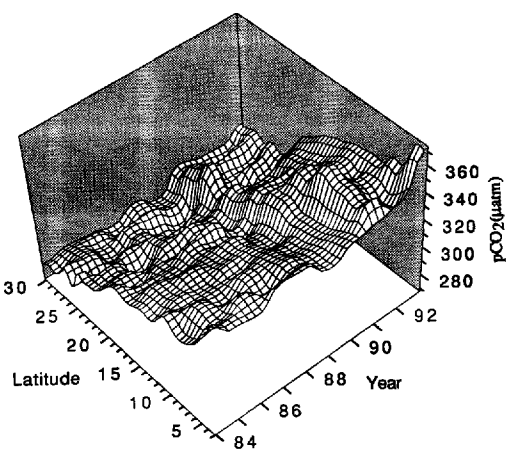

Fig. 6. Variations in normalized pCO_2^{sea} along 137°E during the period from 1984 to 1993. All measurements were made in late January. Effects of interannual changes in SST, salinity and biological activity are normalized to their averages for the period from 1984 to 1993.

annual variability of pCO_2^{sea}: interannual changes of vertical mixing, advection and/or biological activity.

As reported recently, the growth rate of atmospheric CO_2 has decreased considerably since mid-1991 (Keeling et al., 1993, Peterson et al., 1993, Tans et al., 1993). Based on measurements of atmospheric O_2/N_2, enhanced oceanic CO_2 uptake related to the eruption of Mt. Pinatubo, Philippines, has been suggested (Keeling and Manning, 1993; Sarmiento, 1993). However, the distribution and values of pCO_2^{sea} in the western North Pacific close to Mt. Pinatubo, did not change in July 1991 and January 1992.

3.2. *Long-term trend of pCO_2 observed in boreal summer along 137°E and 155°E*

Measurements of pCO_2^{sea} along 137°E and 155°E were made in boreal summer, in 1987 and from 1990 to 1992. Along 137°E, the pattern of pCO_2^{sea} distribution in summer is quite different from that in winter (Inoue and Sugimura, 1992). pCO_2^{sea} increased considerably with increases in the SST due to summer heating of the open ocean waters off southeast Japan (Figs. 7, 8), and in the area of the equatorial counter current and the south equatorial current (Fig. 3) was almost the same as in winter. Near Japan, the pCO_2^{air} decreased due to the photosynthetic activity by land plants (Inoue and Sugimura, 1992). Therefore, the phase of seasonal variation in pCO_2^{sea} is opposite to that of the pCO_2^{air} off the coast of Japan.

Along 155°E, there exists a clear boundary at 25°N (Fig. 7); in the area from 25°N to 31°N, the pCO_2^{sea} increased by 50 μatm from 335 μatm to 385 μatm along with an SST decrease. The pCO_2^{sea} increase was caused by the effects of vertical mixing and biological processes (Takahashi et al., 1993). In the area between 25°N and 5°S, the pCO_2^{sea} ranged from 341 μatm to 355 μatm and tended to slight supersaturation with respect to CO_2 in the overlying air (343–347 μatm). A clear pCO_2^{sea} peak was observed along with a SST peak at 5°N. In this area the pCO_2^{sea} increased by 4.2% along with a 1°C temperature rise.

The pCO_2^{sea} distribution in summer tends to be more variable as compared with the winter season. There are some pCO_2^{sea} peaks north of 20°N along 137°E (Fig. 8), which could be the result of two processes: peaks appeared concomitant with SST

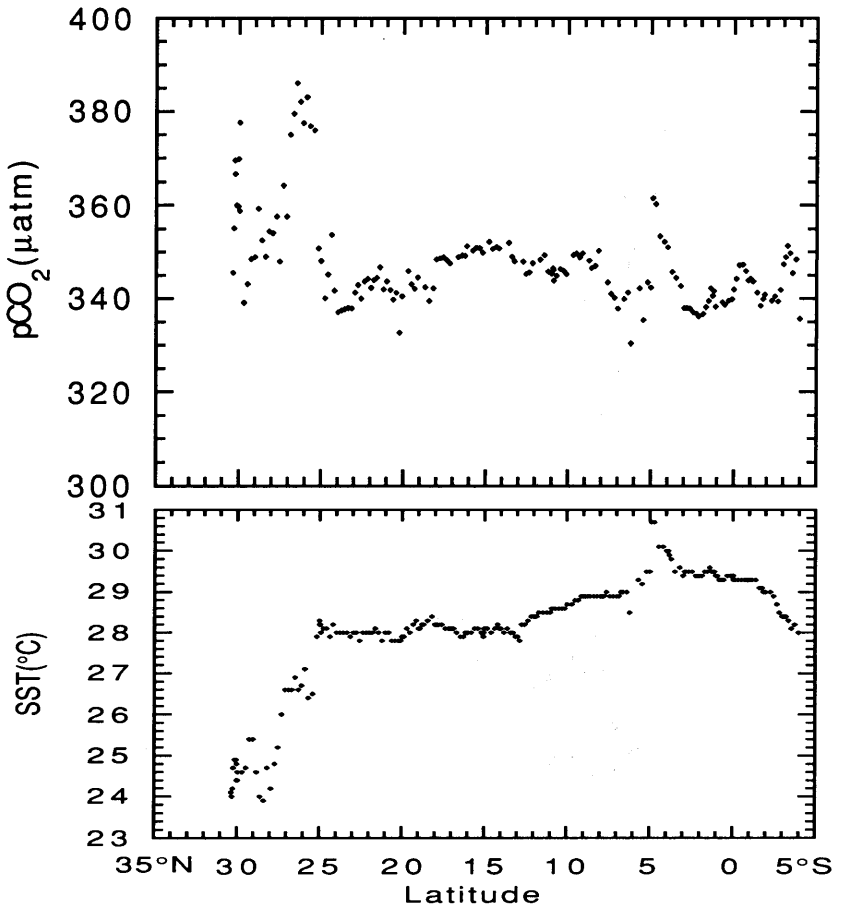

Fig. 7. Latitudinal distribution of pCO_2^{sea} and SST along 155° E in June 1992.

increase or SST decrease. Because measurements of pCO_2^{sea} were made in late July, the mixing layer off the coast of Japan (Fig. 9) was very shallow (less than 30 m north of 21° N in 1990). If the exchange of surface water with subsurface water through the thermocline depends on wind speed as reported by Ryther (1963), this results in pCO_2^{sea} increase with SST decrease. There are some situations in which the pCO_2^{sea} increased with SST. The water temperature close to the air-sea boundary increased due to strong insolation and calm weather conditions. In this case, the pCO_2^{sea} increases with SST during the daytime as observed in the tropical Atlantic (Oudot and Andrié, 1989). Our records at each position are too brief to observe the diurnal pCO_2^{sea} variability. The apparent temperature dependence where pCO_2^{sea} increases with SST is within the range from 3% $°C^{-1}$ to 5% $°C^{-1}$. If pCO_2^{sea} peaks north of 20° N are caused by these phenomena, then repeated measurements over short-time intervals are required to reveal the average pCO_2^{sea} appropriate for use in estimatation of the long-term trends.

Since the vertical mixing of the upper ocean leads to short-term pCO_2^{sea} variability, the growth rate of normalized pCO_2^{sea} was calculated for the transects south of 19° N along 137° E and 20° N along 155° E (Table 2). The SST anomalies in the western equatorial Pacific became almost zero every summer and negative every winter for the period from 1990 to 1993 (Fig. 5). We found that

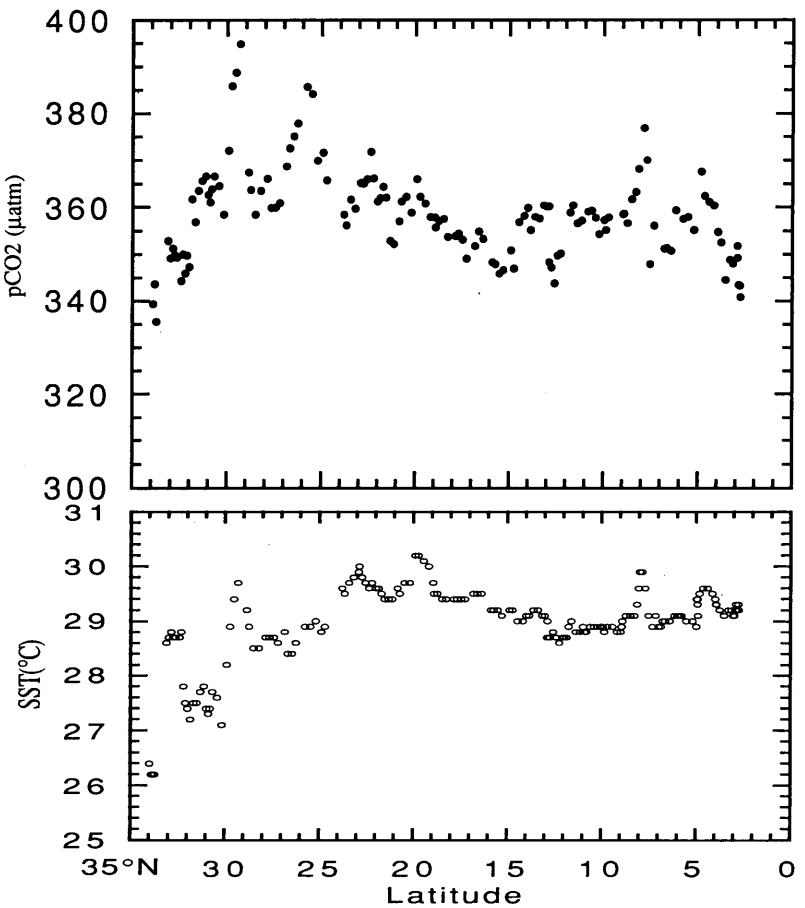

Fig. 8. Latitudinal distribution of pCO_2^{sea} and SST along 137° E in July 1992.

following the end of an El Niño event, the distribution of pCO_2^{sea} changed quickly (Inoue and Sugimura, 1992). Therefore, pCO_2^{sea} measured in summer was expected to show the distribution typical for non-El Niño periods. The rate of pCO_2^{sea} change measured in summer (from -1.5 to $3.6\,\mu atm\,yr^{-1}$) varies from place to place because of the relatively large short-term variations and short duration of observations, but at least the average is positive. The average rate of normalized pCO_2^{sea} change along 137° E and 155° E is calculated to be $1.4 \pm 1.2\,\mu atm\,yr^{-1}$ ($n = 61$, Table 2).

The concentration of atmospheric CO_2 was reported to be nearly constant during the period from 1200 to 1800 (Friedli et al., 1986; Pearman et al., 1986), suggestive of a the steady state for CO_2 exchange between the sea and the air before the industrial era. Due to the CO_2 emissions from human activities, the atmospheric CO_2 concentration has increased from 280 ppm to 353 ppm during the period from 1850 to 1990 (IPCC, 1990). This means that the gross flux from the air to the sea has increased by approximately 26% if the gas transfer coefficient has remained constant. At the moment, changes in net flux from the pre-industrial era to the present is expected to be on the order of $2\,GtC\,yr^{-1}$ (IPCC, 1990). This implies that the gross flux from the sea to the air has also increased by an amount nearly equal to (but slightly less than) the gross flux from the air to the sea. The rate of pCO_2^{sea} increase estimated above is not inconsistent with this expected value.

Under conditions of constant alkalinity, SST

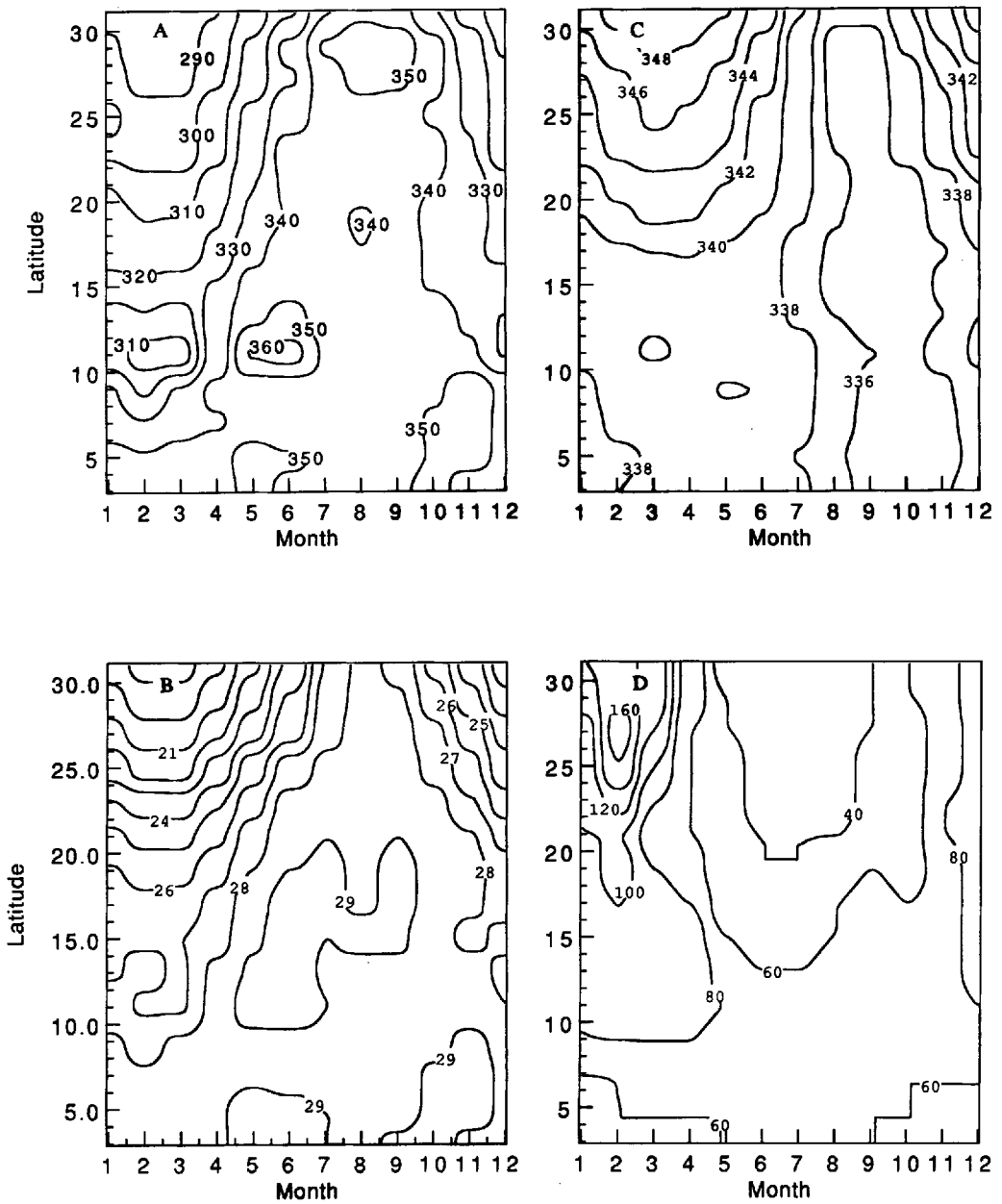

Fig. 9. Seasonal variations in pCO_2^{sea} (A), SST (B), pCO_2^{air} (C), and depth of the mixed layer (D) in 1990. The pCO_2^{sea} and pCO_2^{air} are expressed in μatm, SST in °C, and depth of mixed layer in *m*. The pCO_2^{sea} was evaluated on the basis of the linear relationship between pCO_2^{sea} and SST. The pCO_2^{air} in January 1900 was obtained from the xCO_2^{air} data measured on board. The amplitudes seasonal variation in xCO_2^{air} at every 5°-latitude are taken from the literature (Nakazawa et al., 1992).

and salinity, the rate of TCO_2 increase can be calculated by eq. (1). The apparent rate of pCO_2^{sea} increase leads to a calculated TCO_2 increase of 1 μmol kg^{-1} yr^{-1} north of 15°N and 0.4 μmol kg^{-1} yr^{-1} south of 14°N. As has been reported earlier (see for example, Baes et al., 1985), the transport of carbon to the middle and deep ocean is the rate-limiting step for oceanic CO_2 uptake. Because carbon is not the limiting nutrient for biological activity the marine biota do not directly respond to the increased oceanic CO_2 uptake (IPCC, 1990). The increase of TCO_2 in the mixed layer is caused by the difference in carbon transfer between the air/sea boundary and the surface/middle water boundary. It is of interest to discuss the relationship between the rates of pCO_2^{sea} (and TCO_2) increase and the CO_2 flux between the sea and the air.

3.3. Seasonal pCO_2^{sea} variation in the western North Pacific (132°E–142°E)

In addition to repeated measurements of atmospheric and oceanic pCO_2 along 137°E and 155°E, measurements of pCO_2 have been made for different seasons and positions during the period from November 1983 to July 1993. To characterize the seasonal pCO_2^{sea} variation on the basis of monthly SST data, we investigated the linear relationship between pCO_2^{sea} and SST. No clear changes of longitudinal pCO_2^{sea} distribution were found in the western North Pacific, where each ocean current flows zonally and the contours of monthly SST are almost parallel to longitude lines. Therefore, in this study the pCO_2^{sea} data in the area between 132°E and 142°E were taken to estimate the seasonal variation in pCO_2^{sea}.

Because pCO_2^{sea} in the western equatorial Pacific has increased due to enhanced vertical mixing (Subsection 3.1) every winter for the period from 1991 to 1993, we selected the non-ENSO year, 1990 to examine the seasonal variation in pCO_2^{sea}. To examine the seasonal cycle of the data series it is necessary to remove the long-term increase due to oceanic CO_2 uptake. After removing this trend by approximating the apparent growth rate of pCO_2^{sea} (1.4 μatm/yr) along 137°E, the linear relationship between pCO_2^{sea} and SST was determined for every 1° of latitude by the least squares method (Table 3). In the area north of 30°N, pCO_2^{sea} increased with decreasing SST during the winter season (Inoue et al., 1987; Inoue and Sugimura, 1988) due to vertical mixing, and from winter to summer it increased with SST (the two lines intersects at 19°C). The correlation coefficient varies within the range from 0.63 to 0.98 (Table 3). In the area between the North Equatorial Current and the Kuroshio Counter Current, the correlation coefficient is higher than 0.90, and south of the North Equatorial Current it tends to decrease (0.63–0.94). The low correlation coef-

Table 3. *The linear relationship between pCO_2^{sea} and SST in the western North Pacific (132°E–142°E)*

Latitude N	A (μatm °C^{-1})	B (μatm)	r	No.
31	154.8	6.784	0.948	67
30	157.5	6.658	0.981	50
north of 29*	403.9	−6.334	0.901	55
29	119.4	8.441	0.974	45
28	114.3	8.558	0.946	38
27	123.8	7.989	0.965	37
26	112.9	8.433	0.938	55
25	138.9	7.185	0.899	42
24	109.8	8.194	0.947	29
23	44.56	10.52	0.966	32
22	59.34	9.854	0.952	31
21	88.69	8.746	0.966	36
20	75.51	9.142	0.957	36
19	79.14	8.976	0.963	33
18	22.63	10.91	0.975	28
17	28.48	10.75	0.980	26
16	23.97	10.91	0.975	28
15	76.61	9.192	0.955	24
14	13.43	11.31	0.913	28
13	−89.37	15.02	0.786	38
12	−160.6	17.50	0.687	40
11	−242.5	20.37	0.892	68
10	−244.5	20.39	0.935	31
9	−398.1	25.87	0.962	19
8	−226.8	19.86	0.865	26
7	−219.1	19.56	0.861	32
6	−63.40	14.15	0.687	31
5	47.41	10.37	0.943	29
4	−88.69	14.95	0.936	26
3	−35.33	13.17	0.629	28

Data observed during the period from 1984 to 1993 are used after removing the long-term trend (1.4 μatm yr^{-1}). Data of repeated transects (137°E) are used only in January 1990 and July 1990. The pCO_2^{sea} is given by equation: $pCO_2^{sea} = A(SST) + B$. Numbers of observations (no.) and correlation coefficients (r) are given.

* If SST is lower than 19°C, this relationship was applied.

ficient in the Equatorial Counter Current and the South Equatorial Current is at least partly due to small changes in both pCO_2^{sea} and SST as well as vertical mixing caused by the Mindanao Eddy (Fushimi, 1987). In this area, the interannual variation (20–30 μatm) due to changes in vertical mixing is larger than that due to seasonal variation (10 μatm).

The linear relationship between pCO_2^{sea} and SST allows us to characterize the seasonal variation of pCO_2^{sea} on the basis of monthly mean SST data (Fig. 9). To investigate the processes controlling variation in pCO_2^{sea}, first we estimated the pCO_2^{sea} changes due to thermodynamic processes and air-sea CO_2 flux between two successive months:

$$pCO_2(t+1, x)^{cal} = pCO_2(t, x)^{obs} + \Delta pCO_2^{sst}(t, x) + \Delta pCO_2^{sal}(t, x) + \Delta pCO_2^{Fx}(t, x), \quad (10)$$

$$\partial pCO_2(t+1, x) = pCO_2(t+1, x)^{obs} - pCO_2(t+1, x)^{cal}, \quad (11)$$

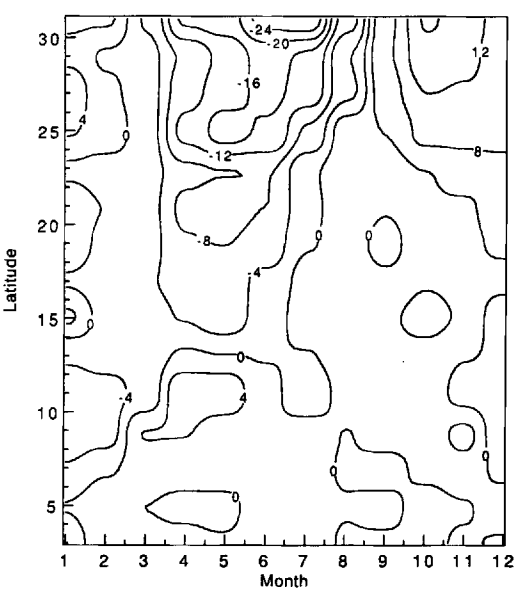

Fig. 10. Seasonal variation in ∂pCO_2 (μatm) in the western North Pacific in 1990. Because ∂pCO_2 is the difference between the observed pCO_2^{sea} changes and those due to thermodynamic processes and CO_2 flux between the sea and the air (see text), ∂pCO_2 reveals the effects of biological activity and mixing dynamics of the upper ocean.

where t is the month, x the latitude, $pCO_2(t, x)^{obs}$ the pCO_2^{sea} estimated from the monthly mean SST data and $pCO_2(t+1, x)^{cal}$ the summation of thermodynamic and air-sea CO_2 flux terms which will be discussed in Subsection 3.5. ∂pCO_2, therefore, represents the effects of lateral water flow, vertical mixing of upper ocean and biological activity on pCO_2^{sea} (Fig. 10). Changes in pCO_2 between successive months due to changes in SST($\Delta pCO_2^{sst}(t, x)$) and salinity ($\Delta pCO_2^{sal}(t, x)$) are estimated by eqs. (2) and (9). Monthly mean salinity was estimated with data from cruises conducted by JMA (JMA, 1990). Gaps between contiguous data were interpolated linearly. The effect of air-sea CO_2 flux on pCO_2 ($\Delta pCO_2^{Fx}(t, x)$) is estimated based on eq. (1) and the assumption that complete mixing occurred quickly in the surface layer. The depth of mixed layer was defined as the depth at which water temperature decreased by 1° from the SST (Lamb, 1984). Seasonal variation in the depth of mixed layer (Fig. 9) is estimated from three cruises along 137°E conducted in January/February, June/July and November 1990, and mixed layer depths reported by Hanawa and Hoshino (1988), Suga and Hanawa (1990), and Fukasawa (private communication).

Generally, the temperature dependence accounts for the largest change in pCO_2^{sea}. ΔpCO_2^{Fx} is a term comparable in size to that of the salinity dependence, and becomes larger in the winter season off the coast of Japan (4–6 μatm eq. (7) used). In the area south of 18°N, ∂pCO_2 is close to 0 μatm, which means that the pCO_2 is controlled mainly by thermodynamic parameters in this subtropical area, as pointed out by Weiss et al. (1982). South of the equatorial counter current there are no clear seasonal changes in ∂pCO_2 (Fig. 10) because the changes in SST and pCO_2^{sea} are small. North of 19°N, a clear seasonal change of ∂pCO_2 occurred: a negative peak occurred from April to August, while a positive one occurred from October to January. The peak-to-trough amplitude increases toward the north. North of 19°N the mixing dynamics and/or biological activity play a relatively more important role in determining temporal change in pCO_2^{sea}. The month when the maximum or minimum δpCO_2 occurred is different from those for ΔpCO_2 and mixed layer depth (Fig. 9). For the period from winter to summer, the depth of the mixed layer decreases and the surface water is incorporated into the deep

water. During the period of thinning of the mixed layer, TCO_2 in the mixed layer may be approximately constant as was assumed by Peng et al. (1987). In contrast, during the period of thickening the mixed layer, TCO_2 is expected to increase due to the incorporation of deep water. The negative ∂pCO_2, therefore, seems to be related to the pCO_2^{sea} decrease by biological activity (CO_2 uptake via photosynthesis). June and July 1990 are the months when the most negative ∂pCO_2 appeared, during which the concentration of $NO_2^- + NO_3^-$ was less than 0.1 μmol kg^{-1} (The Results of Oceanographic Observation, 1990). If no net TCO_2 changes occur due to biological activity, there seem to be two processes affecting pCO_2^{sea}: changes in ratio between organic carbon and $CaCO_3$ formation and/or the usage of HCO_3^- ion for photosynthesis. If phytoplankton use CO_2 taken from the bicarbonate ion during the photosynthesic process and release OH^- ion as in the case of fresh water (Lucas, 1983), this would be an effective process for reducing pCO_2^{sea}. The most positive ∂pCO_2 occurred in October and November when the mixed layer depth was increasing. The addition of TCO_2 due to the incorporation of deep water and respiration of phytoplankton may lead to this boreal autumn maximum. The anti-symmetrical pattern of ∂pCO_2 in the northern region (Fig. 10), could be caused by two processes whose phase and amplitude differ. From the viewpoint of carbonate chemistry, one additional variable (DIC or pH or Alkalinity) is necessary to discuss this point quantitatively. This is a subject for further study.

3.4. *Seasonal ΔpCO_2 variation in the western North Pacific, 132°E–142°E*

To estimate the annual cycle of pCO_2, the monthly mean of xCO_2^{air} in 1990 has been calculated for each degree of latitude by taking into account the long-term trends and seasonal variation. The amplitude of seasonal variation in atmospheric CO_2 was taken from the data reported by Nakazawa et al. (1992). The linear long-term trend was assumed to be 1.8 ppm yr^{-1}, which is the apparent increase rate of atmospheric CO_2 observed every boreal winter. To obtain pCO_2^{air}, water vapor pressure was calculated based on monthly mean SST at 35 psu.

Large negative ΔpCO_2 values (less than -60 μatm) are found off the coast of Japan from January to April. From July to September ΔpCO_2 becomes positive from 31°N to the equator (Fig. 11). The amplitude of seasonal variation shows a clear latitudinal dependence. The maximum amplitude is about 80 μatm in the area between 27°N and 30°N, where the minimum ΔpCO_2 is -60 μatm and the maximum 20 μatm. The amplitude decreases toward the south due mainly to changes in the minimum ΔpCO_2, reaching about 30 μatm at 7°N. The amplitude may drop off further south, but there remain uncertainties derived from the pCO_2/SST relationship. Due to the flatness of the slope near the time when maximum or minimum ΔpCO_2 occur, the months when increasing or decreasing ΔpCO_2 reach 0 μatm are used as indicators of the phase of ΔpCO_2 buildup and drawdown. In the area south of 5°N, ΔpCO_2 is always positive, and tends to be higher during the second half of the year. The buildup of ΔpCO_2 starts at 6°N in February and occurs later to the north. At 30°N, ΔpCO_2 becomes 0 μatm in July. The drawdown starts in October at 30°N, and in December at 10°N. The period in which the ocean acts as a sink for atmospheric CO_2 tends to be longer toward the north.

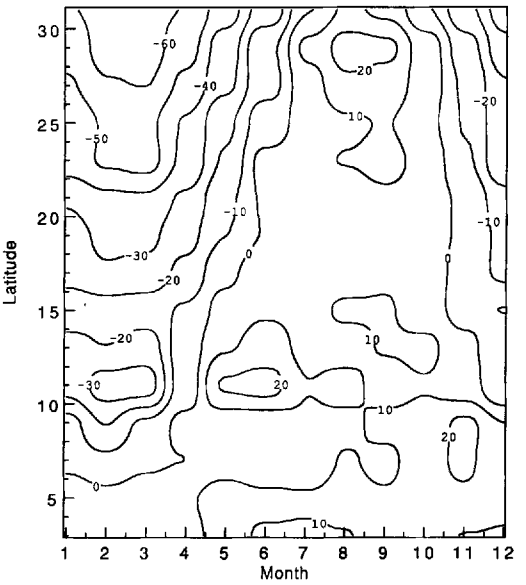

Fig. 11. Seasonal variation in ΔpCO_2 (μatm) in the western North Pacific (132°E–142°E) in 1990. Linear long-term trend of pCO_2^{sea} was added to or subtracted from the pCO_2^{sea} data.

3.5. Oceanic CO_2 uptake

The air-sea CO_2 flux (Fig. 12, Table 4) was computed based on the $\Delta pCO_2^{obs}(t, x)$ and the gas transfer coefficient derived from eqs. (6)–(8). As pointed out previously (Tans et al., 1990), the gas transfer piston velocity by Liss and Merlivat (1986) and Etcheto and Merivat (1988) gives an air-sea CO_2 flux estimate which is almost half that calculated for the same monthly mean of ΔpCO_2 and wind speed. Since our wind speed data are taken from the climatological data set (JMA, 1989), this deviates from calculations which use the in-situ wind speed (Etcheto and Merivat, 1988). Eq. (8) suggested by Wanninkhof (1992) gives a somewhat smaller flux (Table 4) than that calculated with eq. (7).

Because of the large negative ΔpCO_2 and strong wind during the winter season (Fig. 11), off the coast of Japan (north of 27°N), oceanic CO_2 uptake increased to -16 mmol m^{-2} day^{-1} (based on eq. (7), Fig. 12). This area became a weak source during the period from June to October, but the outflux was small (4 mmol m^{-2} day^{-1}) due to the small positive ΔpCO_2 and weak wind speed. Oceanic CO_2 uptake decreases toward the south and the annual mean flux became 0 mmol m^{-2} day^{-1} at 10°N. South of 10°N, the ocean acts as a weak source (0.2–0.7 mmol m^{-2} day^{-1}, annual mean) which is considerably smaller than the fluxes in the central and eastern equatorial Pacific (Feely et al., 1987; Inoue and Sugimura, 1992; Wong et al., 1993; Lefevre and Dandonneau, 1991; Lefevre et al., 1994; Ishii and Inoue, 1995).

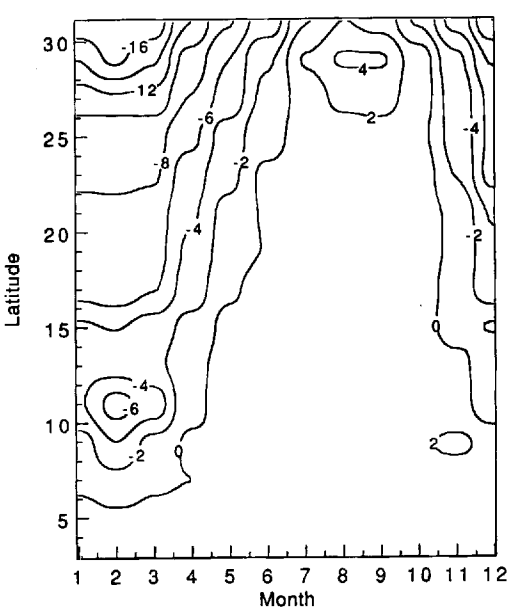

Fig. 12. Seasonal variation in CO_2 flux between the sea and the air (mmol m^{-2} day^{-1}) in 1990. Wind data were taken from the climatological data gathered on cruises between 1971 and 1980. The gas transfer coefficient was given as a function of wind speed (eq. (7)).

Because the amount of TCO_2 transported from the surface layer to the middle/deep water is not known, the increase of TCO_2 (∂TCO_2) is calculated assuming no out-flux from the study area occurred and the stored carbon remainded as inorganic carbon (Table 4). The summation of monthly ∂TCO_2 which are calculated from air-sea CO_2 flux (eq. (7) used), the depth of mixing layer and number of days in one month is given in the last column of Table 4. As discussed above, the TCO_2 (pCO_2) in the mixed layer has been increasing both in the source and sink regions. Carbon exchange between the surface layer and intermediate water in the equatorial Pacific exceeds the outflux of CO_2 in the surface layer. The distribution of ∂TCO_2 reveals trends similar to those observed for the long-term increase of pCO_2, high in the northern region and low in the equatorial region (south of 14°N). However, the magnitude of the calculated long-term TCO_2 trend (0.4–1 μmol kg^{-1} yr^{-1}) is remarkably different from that for ∂TCO_2, especially at 31°N (Table 4). Even if we use eq. (6), there still remains a large difference between the ∂TCO_2 and the calculated TCO_2 increase.

As long as eq. (1) and the air-sea CO_2 flux calculations are valid, the difference between δTCO_2 and the observed TCO_2 increase are caused by carbon transfer from the study area via vertical mixing and/or lateral water transport.

Subtropical mode water is a layer of vertically homogeneous water found between the seasonal thermocline and the deeper main thermocline (Masuzawa, 1969; Bingham, 1992). This water is reported to form in the area just off the Kuroshio south and east of Japan (Suga and Hanawa, 1990). During winter the mixed layers thicken, and becoming thickest in February/March at the end of the cooling season. After the formation of subtropical mode water, it spreads widely throughout the northwestern subtropical gyre (Bingham, 1992). This subtropical mode water could transfer

Table 4. *Annual mean of ΔpCO_2, wind speed (Ws), and CO_2 flux (Fx) along 137° E*

Latitude N	ΔpCO_2 (μatm)	Ws (m s^{-1})	Fx-T (mmol m^{-2} d^{-1})	Fx-L&M (mmol m^{-2} d^{-1})	Fx-W (mmol m^{-2} d^{-1})	∂TCO_2 (μmol kg^{-1} yr^{-1})
31	−31.9	8.1	−8.0	−3.7	−7.3	35.3
29	−22.6	7.7	−5.2	−2.4	−4.5	13.9
27	−21.5	7.2	−4.3	−1.9	−3.6	14.9
25	−18.6	6.9	−3.4	−1.5	−2.8	12.2
23	−16.9	6.8	−2.9	−1.3	−2.4	9.0
21	−11.8	7.0	−2.3	−1.0	−1.9	9.1
19	−9.9	7.3	−2.2	−1.0	−1.9	8.8
17	−7.3	7.5	−2.0	−0.9	−1.8	7.1
15	−0.8	7.3	−0.6	−0.3	−0.6	1.0
13	−1.7	5.4	−0.5	−0.2	−0.4	1.2
11	−1.5	5.5	−1.1	−0.5	−0.8	3.9
9	4.3	5.7	0.2	0.1	0.2	−1.8
7	5.7	5.2	0.4	0.1	0.3	−2.2
5	11.1	4.6	0.7	0.2	0.6	−4.1
3	9.6	4.0	0.4	0.1	0.4	−2.2

∂TCO_2 is the change in TCO_2 due to assuming no net flux between the surface mixed layer and the intermediate/deep water. The summation of monthly ∂TCO_2 derived from eq. (8) is given in the last column. The air-sea CO_2 flux is estimated on the basis of eqs. (7)–(9), where Fx-T refers to eq. (8), Fx-L and M, eq. (7), and Fx-W, eq. (9).

carbon in the surface mixed layer to the intermediate water (Chen, 1982, 1993) around 30° N, the area where a large ∂TCO_2 was found (Table 4). If east of Japan is the predominant area of subtropical mode water formation, lateral water flow could remove carbon from the surface. The seasonal pCO_2^{sea} variability discussed above indicates the importance of biological activity under conditions of low nutrient concentration. It remains for future work to study the relative importance of biological activity versus the mixing dynamics of upper ocean to understand how carbon is accumulated in the western North Pacific.

4. Summary

Since 1981, simultaneous measurements of pCO_2 in the western North Pacific and the overlying air (35° N–0°, 125° E–155° E) have been made. The pCO_2^{sea} was measured along the same transects at the same times of year allow us to estimate the long-term trend caused by air-sea CO_2 flux. During the period from 1984 to 1993, the pCO_2^{sea} at latitudes between 31° N and 3° N increased at an average rate of 1.2 ± 0.9 μatm yr^{-1} ($n = 50$): north of 15° N it rose 1.8 ± 0.6 μatm yr^{-1} ($n = 28$) and south of 14° N 0.5 ± 0.7 μatm yr^{-1} ($n = 22$). North of 15° N the rate of pCO_2^{sea} increase is equal to that of atmospheric CO_2 (1.8 μatm yr^{-1}) during the same period, while south of 14° N it was lower. The mixing dynamics of upper ocean, thermodynamic processes (temperature and salinity), air-sea CO_2 flux, and biological activity are major factors controlling the pCO_2^{sea}. We normalized the observed pCO_2^{sea} by taking into account the effects of thermodynamic processes and biological activity. The normalized pCO_2^{sea} data also show a long-term increase (1.4 ± 0.9 μatm yr^{-1}, $n = 48$) which is close to the apparent increase rate. The increase rate of normalized pCO_2^{sea} also tends to be high north of 15° N, while low in the western equatorial Pacific. The difference in the rate of pCO_2^{sea} increase is suggestive of long-term variation in ΔpCO_2 (pCO_2^{sea}-pCO_2^{air}) as indicated by carbon cycle models (Volk and Bacastow, 1989). However, there remain large uncertainties concerning the pCO_2^{sea} increase due to the increased CO_2 influx because of large short-term and interannual variations.

In addition to the repeated measurements, we have conducted pCO_2 measurements in the western North Pacific for different seasons during the period from 1983 to 1993. After removing the long-term trend, the seasonal variations in pCO_2^{sea} in the western North Pacific (132° E–142° E) were evaluated for each latitude based on the

relationship between pCO_2^{sea} and sea surface temperature (SST). Most of the correlation coefficients were higher than 0.90 (range from 0.63 to 0.98), and they tended to be low south of 7°N where clear seasonal variation was not found. In the subtropics (18°N–7°N), thermodynamic processes play a predominant role in determining the seasonal variation of pCO_2^{sea} (Weiss et al., 1982). The pCO_2^{sea} north of 19°N was affected by biological activity and vertical mixing, and their effects increased toward the north.

The annual CO_2 flux between the sea and the air was estimated based on monthly mean ΔpCO_2 and the gas transfer coefficient calculated according to Liss and Merlivat (1986), Tans et al. (1990) and Wanninkhof (1992). Large influxes of CO_2 occurred off the coast of Japan (-16 mmol m^{-2} day^{-1}, based on Tans et al. (1990)) because of the large negative ΔpCO_2 (-60 μatm) and strong wind during the winter season. In the sink area, the annual mean air-sea CO_2 flux ranged from -8 mmol m^{-2} day^{-1} at 31°N to -1 mmol m^{-2} day^{-1} at 11°N. The increase rate of pCO_2^{sea}, therefore, is high in the region where ocean acts as a strong sink for atmospheric CO_2. South of 10°N the ocean acts as a source (0.2–0.7 mmol m^{-2} day^{-1}). But, outflux of CO_2 is considerably smaller compared with those in the central and eastern equatorial Pacific (Feely et al., 1987; Inoue and Sugimura, 1992; Wong et al., 1993; Lefevre and Dandonneau, 1991; Lefevre et al., 1994; Ishii and Inoue, 1995).

The long-term trend of pCO_2^{sea} gives the rate of dissolved inorganic carbon concentration (TCO_2) increase via the buffer factor. The observed increase of pCO_2^{sea} and estimated air-sea CO_2 flux suggest that TCO_2 in the mixed layer could increase by several fold if no out-flux from the mixed layer occurred. The removal of carbon from the mixed layer should be large off the coast of Japan. Subtropical Mode Water formation south of the Kuroshio Current and east of Japan (Suga and Hanawa, 1990) is a candidate mechanism for the rapid transfer of carbon from the mixed layer to the intermediate/deep water (Chen, 1982, 1993). Biological activity may play an important role in determining pCO_2-TCO_2 relationship by changing pH via the photosynthesis/respiration and $CaCO_3$ formation reactions.

5. Acknowledgments

We thank the officers and crews of the R. V. Ryofu-maru (JMA), the R. V. Natsushima (Japan Marine Science and Technology Center), R. V. Kaiyo (Japan Marine Science and Technology Center), the R. V. Hakuho-maru (Ocean Research Institute, Tokyo University), the M. V. Yashirogawa-maru (Kawasaki Kisen Co. Ltd.), the M. V. Wellington-maru (Osaka Shosen Mitsui Co. Ltd.) for their help on board. We wish to express particular appreciation to the JMA, Science and Technology Agency, and Environmental Agency for finical support of this research. We also thank anonymous reviewers and Dr. R. Weisburd (National Institute for Environmenta Studies) for their helpful discussions and suggestions.

REFERENCES

Baes, Jr, C. F., Björkström, A. and Mulholland, P. J. 1985. Uptake of carbon dioxide by the oceans. In: *Atmospheric carbon dioxide and the global carbon cycle.* DOE/ER-0239. (ed. J. R. Trabalka). Washington. 81–111.

Bingham, F. M. 1992. Formation of spreading subtropical mode water in the North Pacific. *J. Geophys. Res.* **97**, 11177–11189.

Broecker, W. S., Ledwell, J. R., Takahashi, T., Weiss, R., Merlivat, L., Memery, L., Peng, T. H., Jahne, B. and Munnich, K. O. 1986. Isotopic versus micrometeorologic ocean CO_2 fluxes: A serious conflict. *J. Geophys. Res.* **88(C7)**, 4343–4354.

Chen, C. T. 1982. Oceanic penetration of excess CO_2 in a cross-section between Alaska and Hawaii. *Geophys. Res. Lett.* **9**, 117–119.

Chen, C. T. 1993. The oceanic anthropogenic CO_2 sink. *Chemosphere* **27**, 1041–1064.

Etcheto, J. and Merlivat, L. 1988. Satellite determination of the carbon dioxide exchange coefficient at the ocean-atmosphere interface: a first step. *J. Geophys. Res.* **93**, 15699–15678.

Feely, R. A., Gammon, R. H., Taft, B. A., Pullen, P. E., Waterman, L. S., Conway, T. J., Gendron, J. F. and Wisegarver, D. P. 1987. Distribution of chemical tracers in the eastern equatorial Pacific during and

after the 1982–83 El Niño/Southern Oscillation Event. *J. Geophys. Res.* **92**, 6545–6558.

Friedli, H., Lötscher, H., Oeschger, H., Siegenthaler, U. and Staufer, B. 1986. Ice core record of the $^{13}C/^{12}C$ ratio of atmospheric CO_2 in the past two centuries. *Nature* **324**, 237–238.

Fushimi, K. 1987. Variation of carbon dioxide partial pressure in the western North Pacific surface water during the 1982/83 El Niño Event. *Tellus* **39B**, 214–227.

Gordon, L. I. and Jones, L. B. 1973. The effect of temperature on carbon dioxide partial pressure in seawater. *Mar. Chem.* **1**, 317–322.

Goyet, C. and Pelzer, E. T. 1994. Comparison of the August–September 1991 and 1979 surface partial pressure of CO_2 distribution in the equatorial Pacific Ocean near 150° W. *Mar. Chem.* **45**, 257–266.

Hanawa, K. and Hoshino, I. 1988. Temperature structure and mixed layer over the Izu Ridge. *J. Mar. Res.* **46**, 683–700.

Hirota, M., Nemoto, K., Murata, A. and Fushimi, K. 1991. Observation of carbon dioxide in air and surface seawater in the western North Pacific Ocean. *Oceanographical Mag.* **41**, 19–28.

Inoue, H., Sugimura, Y. and Fushimi, K. 1987. pCO_2 and $\delta^{13}C$ in the air and surface sea water in the western North Pacific. *Tellus* **39B**, 228–242.

Inoue, H. and Sugimura, Y. 1988a. Distribution and variations of oceanic carbon dioxide in the western North Pacific, eastern Indian, and Southern Ocean south of Australia. *Tellus* **40B**, 308–320.

Inoue, H. and Sugimura, Y. 1988b. Distribution of the pCO_2 in surface seawater of the western and central equatorial Pacific during the 1986/87 El Niño/Southern Oscillation event. *Geophys. Res. Lett.* **15**, 1499–1502.

Inoue, Y. H. and Sugimura, Y. 1992. Variations and distributions of CO_2 in and over the equatorial Pacific during the period from the 1986/88 El Niño event to the 1988/89 La niña event. *Tellus* **44B**, 1–22.

Inter-Governmental Panel on Climate Change. 1990. Greenhouse gases and Aerosols. In: *Climate change. The IPCC scientific assessment.* (eds. Houghton, J. T., Jenkins, G. J. and Ephraums, J. J.). Cambridge University Press. Cambridge, pp. 5–40.

Ishii, H., Sekine, Y. and Toba Y. 1983. Hydrographic structure of the Kuroshio large meander-cold water mass region down to the deeper layers of the ocean. *J. Oceanogr. Soc. Japan.* **39**, 240–250.

Ishii, M. and Inoue, H. Y. 1995. Air-sea exchange of CO_2 in the central and western equatorial Pacific in 1990. *Tellus* **47B**, 447–460.

Japan Meteorological Agency. 1989. *Marine climatological tables of the North Pacific Ocean for 1971-1980.* Marine Department, JMA. Tokyo.

Kawabe, M. 1990. A steady state model of typical non-large-meander paths of the Kuroshio Current. *J. Oceanogr. Soc. Japan* **46**, 55–67.

Keeling, C. D. 1968. Carbon dioxide in surface ocean waters (4). Global distribution. *J. Geophys. Res.* **73**, 4543–4553.

Keeling, C. D., Bacastow, R. B., Carter, A. F., Piper, S. C., Whorf, T. P., Heimann, T. P., Mook, W. G. and Roeloffozen, H. 1989. A three-dimensional model of atmospheric CO_2 transport based on observed winds (1). Analysis of observational data. In: *Aspect of climate variability in the Pacific and western America* (ed. D. M. Peterson). AGU Geophysical Monograph. Washington DC, pp. 165–236.

Keeling, C. D. and Whorf, T. 1993. Trends in atmospheric CO_2 since the eruption of Pinatubo in 1991. *World Meteorological Organization Global Atmospheric Watch (4th CO_2 International Conference)*, pp. 19.

Lamb, P. J. 1984. On the mixed layer climatology of the north and tropical Atlantic. *Tellus* **36A**, 292–305.

Lefevre, N. and Dandonneau, Y. 1992. Air-sea CO_2 exchange in the equatorial Pacific in January–March 1991. *Geophys. Res. Lett.* **19**, 2223–2226.

Lefevre, N., Andrié, C., Dandonneau, Y., Reverdin, G. and Rodier, M. 1994. PCO_2, chemical properties, and estimated new production in the equatorial Pacific in January–March 1991. *J. Geophys. Res.* **99(C6)**, 12639–12654.

Liss, P. S. and Merlivat, L. 1986. Air-sea gas exchange rates: introduction and synthesis. In: *The rôle of air-sea exchange in geochemical cycling* (ed. P. Buat-Menard). Dordrecht, Holland: D. Reidel, 113–127.

Lucas, W. J. 1983. Photosynthetic assimilation of exogenous HCO_3^- by aquatic plants. *Ann. Rev. Plant Physiol.* **34**, 71–104.

Masuzawa, J. 1969. Subtropical mode water. *Deep Sea Res.* **16**, 463–472.

Miyake, Y., Sugimura, Y. and Saruhashi, K. 1974. The carbon dioxide content in the surface water in the Pacific Ocean. *Rec. Oceanogr. Wks. Japan.* **12**, 45–52.

Monthly Ocean Report. 1993. El Niño Monitoring Center, JMA. Tokyo.

Murphy, P. P., Feely, R. A. and Gammon, R. H. 1993. *Interannual variability of ΔpCO_2 in the North Pacific.* World Meteorological Organization Global Atmospheric Watch (4th CO_2 International Conference), pp. 78.

Nakazawa, T., Murayama, S., Miyashita, K., Aoki, S. and Tanaka, M. 1992. Longitudinally different variations of lower tropospheric carbon dioxide concentrations over the North Pacific Ocean. *Tellus* **44B**, 161–172.

Oudot, C. and Andrié, C. 1989. Short-term changes in the partial pressure of CO_2 in eastern tropical Atlantic surface seawater and in atmospheric CO_2 mole fraction. *Tellus* **41B**, 537–553.

Pearman, G. I., Etheridge, D., de Silva, F. and Fraser, P. J. 1986. Evidence of changing concentrations of atmospheric CO_2, N_2O, and CH_4 from air bubbles in Antarctic ice. *Nature* **320**, 248–250.

Peterson, J. T., Thoning, K. W. and Tans, P. P. 1993. Continuous atmospheric carbon dioxide measure-

ments at Barrow, Alaska, 1973–1992. *World Meteorological Organization Global Atmospheric Watch (4th CO_2 International Conference)*, pp. 2.

Peng, T. H., Takahashi, T., Broecker, W. S. and Olafsson, J. 1987. Seasonal variability of carbon dioxide in the northern North Atlantic surface water: observations and a model. *Tellus* **39B**, 439–458.

Revelle, R. and Suess, H. E. 1957. Carbon dioxide exchange between atmosphere and ocean, and the question of an increase of atmospheric CO_2 during the past decades. *Tellus* **9**, 18–27.

Ryther, J. H. 1963. Biological oceanography. In: *The sea*, vol. 2. (ed. M. N. Hill). New York. John Wiley & Sons, pp. 347–380.

Suga, T. and Hanawa, K. 1990. The mixed-layer climatology in the northwestern part of the North Pacific subtropical gyre and the formation area of Subtropical Mode Water. *J. Marine Res.* **48**, 543–566.

Sundquist, E. T., Olummer, L. N. and Wigley, T. M. L. 1979. Carbon dioxide in the ocean surface: the homogeneous buffer factor. *Science* **204**, 1203–1205.

Takahashi, T., Olafsson, J., Goddard, J. G., Chipman, D. W. and Sutherland, S. C. 1993. Seasonal variation of CO_2 and nutrients in the high-latitude surface oceans. A comparative study. *Global. Biogeochem. Cycles* **7**, 843–878.

Tanaka, M., Nakazawa, T. and Aoki, S. 1987. Time and space variations of tropospheric carbon dioxide over Japan. *Tellus* **39B**, 3–12.

Tans, P. P., Fung, I. and Takahashi, T. 1990. Observational constrains on the global atmospheric CO_2 budget. *Science* **247**, 1431–1438.

Tans, P. P., Conway, T. J., Kitzis, D. R., Masarie, K. A., Stavisch, M., Waterman, L. S., White, J. C. and Zhang, Ni. 1993. Evidence for interannual variability of the carbon cycle from measurements of the CMDL Cooperative Global Flask Network. *World Meteorological Organization Global Atmospheric Watch (4th CO_2 International Conference)*, pp. 10.

The Results of Oceanographic Observations, 1990. Japan Meteorological Agency. Tokyo.

Volk, T. and Bacastow, R. 1989. The changing patterns of ΔpCO_2 between ocean and atmosphere. *Global Biogeochem. Cycles* **3**, 179–189.

Wagner, K. 1979. The carbonate system of the ocean. In: *The global carbon cycle* (eds. Bolin, B., Degens, E. T., Kempe, S. and Ketner, P.). Chichester. John Wiley & Sons, 251–258.

Wanninkhof, R. 1992. Relationship between wind speed and gas exchange over the ocean. *J. Geophys. Res.* **97**, 7373–7382.

Weiss, R. 1974. CO_2 in water and sea water: the solubility of a non ideal gas. *Mar. Chem.* **2**, 203–215.

Weiss, R. F., Jahnke, R. A. and Keeling, C. D. 1982. Seasonal effects of temperature and salinity on the partial pressure of CO_2 in sea water. *Nature* **300**, 511–513.

Wong, C. S. and Chan, Y.-H. 1991. Temporal variations in the partial pressure and flux of CO_2 at ocean station P in the subarctic northeast Pacific Ocean. *Tellus* **43B**, 206–223.

Wong, C. S., Chan, Y.-H., Page, J. S., Smith, G. E. and Bellegay, R. D. 1993. Changes in equatorial CO_2 flux and new production estimated from CO_2 and nutrient levels in Pacific surface waters during the 1986/87 El Niño. *Tellus* **45B**, 64–79.